Neural Networks 176 (2024) 106329

Contents lists available at ScienceDirect

Neural Networks

journal homepage: www.elsevier.com/locate/neunet

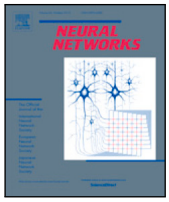

Full Length Article

The role of directed cycles in a directed neural network

Qinrui Dai [a], Jin Zhou [a,b,*], Zhengmin Kong [c]

[a] School of Mathematics and Statistics, Wuhan University, Hubei 430072, China
[b] Hubei Key Laboratory of Computational Science, Wuhan University, Hubei 430072, China
[c] School of Electrical Engineering and Automation, Wuhan University, Hubei 430072, China

ARTICLE INFO

Keywords:
Directed acyclic network
Neural network
Stability
Hopf bifurcation
Cycle

ABSTRACT

This paper investigates the dynamics of a directed acyclic neural network by edge adding control. We find that the local stability and Hopf bifurcation of the controlled network only depend on the size and intersection of directed cycles, instead of the number and position of the added edges. More specifically, if there is no cycle in the controlled network, the local dynamics of the network will remain unchanged and Hopf bifurcation will not occur even if the number of added edges is sufficient. However, if there exist cycles, then the network may undergo Hopf bifurcation. Our results show that the cycle structure is a necessary condition for the generation of Hopf bifurcation, and the bifurcation threshold is determined by the number, size, and intersection of cycles. Numerical experiments are provided to support the validity of the theory.

1. Introduction

Directed acyclic networks are common in the real-world, which do not contain directed cycles (rings) (Bang-Jensen & Gutin, 2008; Jiang, Zhou, Small, Lu, & Zhang, 2023; Williams, Bach, Matthiesen, Henriksen, & Gagliardi, 2018), such as directed chains, directed grids and directed star-chains. A great number of scholars are committed to the dynamics of these directed acyclic networks, mainly involving synchronization and consensus performance (Panteley & Loría, 2017; Papachristodoulou, Jadbabaie, & Münz, 2010; Zhou, Chen, Lu, & Lü, 2016; Zhu, Zhou, Yu, & Lu, 2020a, 2020b). For example, Zhang, Chen, and Mo (2017) investigated the effect of adding a reverse edge to the consensus of directed $1D$ chain and directed $2D$ grid, and concluded that the reverse edge would decrease the dominant convergence rate of the network. Subsequently, Hao, Wang, Duan, and Chen (2019) discussed the effect of adding two reverse edges on the consensus of the directed chain based on Zhang et al. (2017), and found that the consensus performance would not be enhanced when the second reverse edge is added.

However, these results only studied the consensus of simple directed chains, and did not get a general conclusion about directed acyclic graph networks. On the one hand, various dynamics of this type of networks should be further investigated beyond synchronization and consensus. For instance, stability and bifurcation are important tools for exploring complex systems and networks (Chen, Xiao, Wan, Huang, & Xu, 2021; Tao, Xiao, Zheng, Cao, & Tang, 2020; Wang, Zhao, & Cao, 2016), which focus on the dynamics of systems when parameters are continuously changed (Song, Han, & Wei, 2005; Wang & Jian, 2010; Xu, Cao, Xiao, Ho, & Wen, 2014). Among single parameter bifurcations, Hopf bifurcation is extensively explored since it demonstrates the dynamic phenomenon from point to limit cycle in phase plane(Guo, 2022; Wu, Zhang, & Feng, 2021). Recently, with further research of bifurcation on nonlinear systems, bifurcation control (Chen, Hill, & Yu, 2003; Jiang, Chen, Huang, & Yan, 2020; Wang, Wang, & Xia, 2019) has been proposed to observe the dynamics of controlled parameterized systems, such as time delay self-feedback control (Premraj, Suresh, Banerjee, & Thamilmaran, 2017), hybrid control (Yuan & Yang, 2015) and stochastic control (Xu, Ma, & Zhang, 2011). On the other hand, the complexity of directed acyclic networks in the real world is much higher than that of directed chain. The innate character of dynamics in modified directed acyclic networks should also be studied rather than considering only one edge adding operation on special networks (Liu, Xie, Shi, & Yao, 2022; Mo, Chen, & Zhang, 2019). Neural networks are a particular class of complex networks with the capability of signal processing that has become a hot research topic in computer science and engineering (Awodele & Jegede, 2009; Guan, Lai, Li, Yang, & Gu, 2022; Jiang, Xiong, & Shi, 2021). Nevertheless, currently most neural network models are given in advance (Peng & Song, 2009; Xu, Tang, & Liao, 2011), and there is little specific research on their structure, which makes it difficult to design a suitable model based on practical requirements. Thus, it is worth paying attention to which edge adding method can maintain or improve the local dynamics of directed acyclic neural networks and which structure plays a significant role in the dynamics of the neural networks.

* Corresponding author at: School of Mathematics and Statistics, Wuhan University, Hubei 430072, China.
E-mail address: jzhou@whu.edu.cn (J. Zhou).

https://doi.org/10.1016/j.neunet.2024.106329
Received 8 August 2023; Received in revised form 9 March 2024; Accepted 17 April 2024
Available online 19 April 2024

Based on the above discussion, we sum up the main innovation and contribution of this paper as follows.

1. We propose edge adding control on a delayed directed acyclic neural network with arbitrary structure to investigate the improvement of network dynamics. Time delay is selected as a key parameter to study the stability and Hopf bifurcation of the network.
2. It is found that the emergence of directed cycles is the decisive factor in the dynamic changes of the network. The edge adding operations maintain the stability of the network when there is no directed cycle, while the Hopf bifurcation may occur when there is at least one directed cycle. That is to say, the cycle structure is a necessary condition for the generation of Hopf bifurcation.
3. Cycles with the same number and size have a consistent effect on the local stability and Hopf bifurcation of the network, regardless of the number and position of the added edges. The Hopf bifurcation threshold is affected by the number, size, and intersection of the cycles.

In the theoretical analysis, we use the Coates flow graph to further broaden the application scope of theoretical calculation, then obtain more detailed sufficient conditions to estimate the network stability and the existence of Hopf bifurcation. In addition, previous studies have lacked attention to the structure of neural network models, with most of them being given network structures, such as quaternion neural network (Wang & Jian, 2010) and ring neural network (Tao et al., 2020). Therefore, the existing results are only applicable to a few models and have certain limitations. However, starting from searching for the key structure of a neural network, we derive the necessary conditions for the generation of Hopf bifurcation in the network, and analyzed the factors that affect the threshold of Hopf bifurcation.

The rest of the paper is arranged as follows. Section 2 provides some mathematical preliminaries and definitions. In Section 3, we design an edge adding control on a directed acyclic neural network, and investigate the local stability and Hopf bifurcation of the controlled network under different directed cycles. In Section 4, some numerical examples are given to verify the validity of the theory. Finally, a brief conclusion and summary section completes the paper.

2. Preliminaries and definitions

Lemma 1 (*Desoer, 1960*). *For a square matrix Q of n-order corresponding to the flow graph G, one has*

$$\det Q = \sum_{i=1}^{p} (-1)^{n+n_i} G_i,$$

where p represents the number of subgraphs for G, each consisting of non-contact loops of n nodes. n_i and G_i are the number of directed loops and the product of the connection gains of each edge in the ith subgraphs ($i = 1, \dots, p$). (See Fig. 1).

Definition 1. A node is called the root node (leader node) of a directed acyclic network if it does not receive information from other nodes.

Definition 2. When adding a directed edge to a directed acyclic graph, the start node of the edge is called the head node, and the end node is called the tail node.

Definition 3. A directed cycle of length l is defined as a directed closed loop containing l nodes $\{n_1, n_2, \dots, n_l\}$ and l directed edges $(n_1, n_2), (n_2, n_3), \dots, (n_l, n_1)$. The size of the directed cycle refers to the number of nodes on it.

Definition 4. For k directed cycles, if any one intersects with the remaining $k-1$ cycles but does not coincide, then k cycles are called fully intersected cycles.

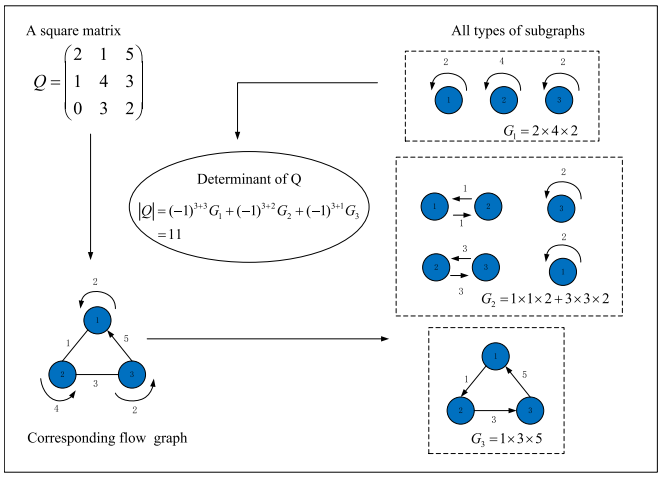

Fig. 1. A 3-order matrix and its corresponding subgraphs.

3. Directed neural network

Consider a directed acyclic neural network with time delay as

$$\dot{x}_i(t) = -a_i x_i + \sum_{j=1}^{n} b_{ij} f_{ij}(x_j(t-\tau)), \tag{1}$$

where x_i is the state of the ith neuron at time t, $a_i > 0$ ($i = 1, 2, \dots, n$) the self-feedback coefficient of the ith neuron, b_{ij} the connection weight between neurons j and i ($b_{ij} = 0$ if no directed edge from j to i), and τ the time delay. $f_{ij}(\cdot)$ denotes the activation function satisfying $f_{ij}(\cdot) \in C^1$ and $f_{ij}(0) = 0$, $f_{ij}'(0) \neq 0$. Note that the structure of network (1) can be arbitrary, and unnecessarily contain a spanning tree.

According to Lemma 1, it is easy to know that the characteristic equation of the Jacobian matrix of network (1) at the zero equilibrium point is given by

$$\prod_{i=1}^{n} (\lambda + a_i) = 0, \tag{2}$$

which shows $\lambda_i = -a_i$ ($i = 1, 2, \dots, n$).

Remark 1. The zero equilibrium point is trivial for neural network models, which means that most network models have the zero equilibrium point and not necessarily the non-zero equilibrium points. Therefore, the stability analysis results of the zero equilibrium point have a wider applicability. Moreover, the non-zero equilibrium points can be transformed into the zero equilibrium point through a linear transformation. For example, for system $\dot{\xi} = F(\xi)$ with non-zero equilibrium point $E_1(\xi^*)$, consider the following linear transformation

$$\tilde{\xi} = \xi - \xi^*,$$

then system $\dot{\tilde{\xi}} = F(\tilde{\xi} + \xi^*)$ have zero equilibrium point $E_0(0)$. For this reason, the stability and bifurcation analysis of the non-zero equilibrium point of $\dot{\xi} = F(\xi)$ are equivalent to that of the zero equilibrium of $\dot{\tilde{\xi}} = F(\tilde{\xi} + \xi^*)$.

Accordingly, we have the following conclusion for directed acyclic network (1).

Lemma 2. *For any $\tau \geq 0$, network (1) will not undergo Hopf bifurcation due to real numbers a_i ($i = 1, 2, \dots, n$), and its zero equilibrium point is always stable when all $a_i > 0$.*

Proof. Due to the eigenvalues of the Jacobian matrix of network (1) being $\lambda_i = -a_i$ ($i = 1, 2, \dots, n$), there is no pair of pure virtual eigenvalues. Therefore, the network will not undergo Hopf bifurcation.

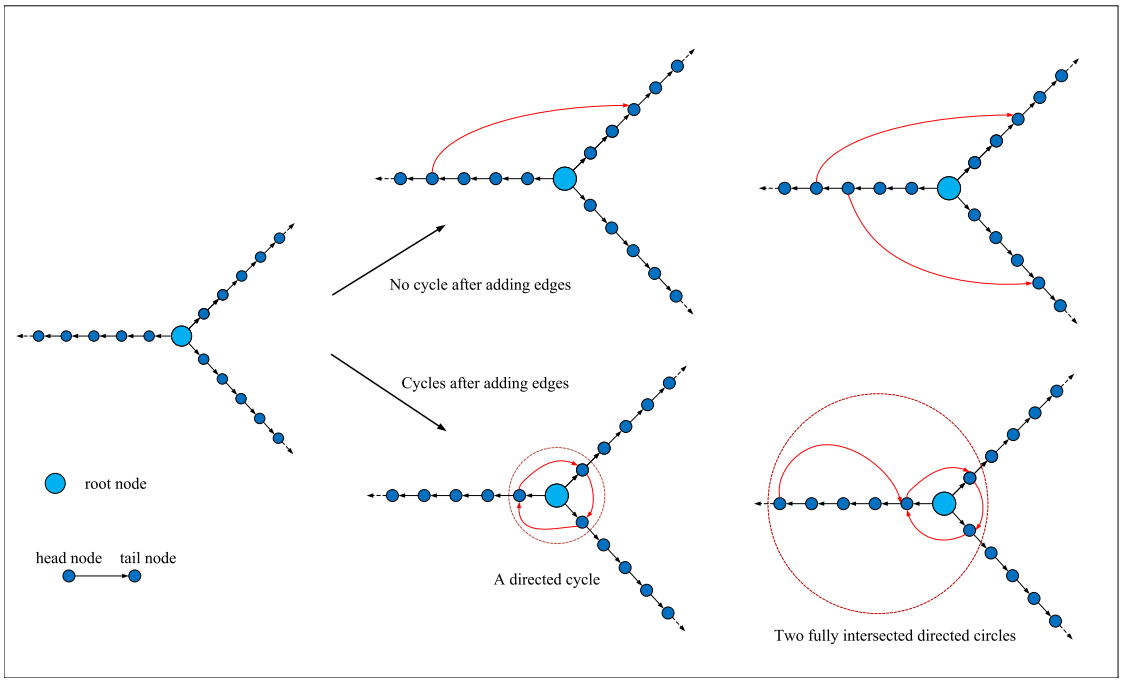

Fig. 2. Adding edge of a directed star-chain network with three chains.

In addition, if $a_i > 0$, then all eigenvalues of the Jacobian matrix of the network have negative real parts, that is, the zero equilibrium point is asymptotically stable.

Now we attempt to improve the dynamic properties of network (1) by edge adding control, and obtain the following controlled network

$$\dot{x}_i(t) = -a_i x_i(t) + \sum_{j=1}^{n} b_{ij} f_{ij}(x_j(t-\tau)) + u_i(t), \tag{3}$$

in which $u_i(t)$ denotes the edge adding controller. For example, if a directed edge from neuron k to neuron i is added, then $u_i(t) = b_{ik} f_{ik}(x_k(t-\tau))$.

Remark 2. Edge adding operation is an effective method for identifying key structures that affect network dynamics, and it has been widely applied in studying network consensus (Hao et al., 2019; Jiang et al., 2023; Zhang et al., 2017). Therefore, the control strategy of Eq. (3) is aimed at investigating which structure can determine the dynamics of directed neural networks.

Theorem 1. *If there is no directed cycle in edge adding network (3), then the characteristic equation of its Jacobian matrix at the zero equilibrium point is the same as that of network (1), that is, this edge adding control does not improve the local dynamics of the original network.*

Proof. Since there is no cycle in edge adding network (3), the characteristic equation of Jacobian matrix of network (3) at the zero equilibrium point is also given by Eq. (2), that is, the edge adding operation without cycle structure does not affect the local dynamics of the network.

Theorem 2. *The characteristic equation of Jacobian matrix of network (3) at the zero equilibrium point is determined by the size and number of its cycles, as well as whether they intersect, and is independent of the number and position of the added edges.*

Proof. According to Lemma 1, the characteristic equation of a matrix is only determined by the size and number of non-contact loops in its corresponding flow graph. Hence, for a directed acyclic network, if different added edges make the network have the same number and size of directed cycles, then the effect of these edges on the characteristic equation is consistent.

Assumption 1. The self-feedback coefficient and connection weight of network (1) are unified, namely $a_i = a$, $b_{ij} f_{ij}'(0) = b$ for $i, j = 1, 2, \ldots, n$.

Fig. 2 shows two edge adding strategies, one that does not form a directed cycle, and the other that forms cycles. In the following two subsections, under the condition of Assumption 1, we investigate the impact of different cycles on the stability and bifurcation of the network.

3.1. Adding edges forms one cycle

Given that the edge adding control makes network (3) form a cycle with p nodes, then according to Lemma 1, the characteristic equation of Jacobian matrix of network (3) at the zero equilibrium point is

$$(\lambda + a)^n + (-1)^{2n-p+1}(-1)^p(\lambda + a)^{n-p} b^p e^{-\lambda p\tau} = 0,$$

and further, by multiplying $e^{\lambda n\tau}$ on both sides of the above equation, we have

$$\left[(\lambda + a)e^{\lambda\tau}\right]^{n-p} \left\{ \left[(\lambda + a)e^{\lambda\tau}\right]^p - b^p \right\} = 0. \tag{4}$$

The following two cases are discussed in the light of whether the time delay τ is zero.

Case I: $\tau = 0$. On this condition, characteristic Eq. (4) is rewritten as

$$(\lambda + a)^{n-p} \left\{ (\lambda + a)^p - b^p \right\} = 0. \tag{5}$$

Therefore, we have the following conclusions.

Lemma 3. *For $b > 0$, if $a > b$ is satisfied, then the zero equilibrium point of network (3) without delay is asymptotically stable; it is unstable when $a < b$ holds.*

Proof. On the one hand, Eq. (5) has $n - p$ real roots, which are all negative for $a > 0$. On the other, the residual root of Eq. (5) is

determined by

$$s^p - b^p = 0, \tag{6}$$

where $s = \lambda + a$. Hence, we can obtain all the roots of Eq. (6) on the complex plane for $b > 0$,

$$s_j = \lambda_j + a = be^{\mathrm{i}\theta} = b(\cos\theta_j + \mathrm{i}\sin\theta_j),$$

with $\theta_j = (2j\pi)/p$, $j = 0, 1, \ldots, p-1$. Apparently, s_0 is the root with the largest real part among all s_j, illustrating $\mathrm{Re}(\lambda_j) \le \mathrm{Re}(\lambda_0) = \mathrm{Re}(s_0) - a = b - a < 0$ for all $j = 0, 1, \ldots, p-1$, when $a > b$ holds. Thus, if $b > 0$ and $a > b$, then all roots of Eq. (5) have negative real parts, that is, the zero equilibrium point of network (3) is asymptotically stable. Moreover, if $a < b$, then Eq. (6) obviously has a positive root λ_0, that is, the zero equilibrium point is unstable.

Lemma 4. *If $b < 0$, the following conclusions hold true.*

1. *For an odd number p, the solution of non-delay network (3) is stable when $a > -b\cos(\pi/p)$, and unstable when $a < -b\cos(\pi/p)$.*
2. *For an even number p, the solution of non-delay network (3) is stable when $a > -b$, and unstable when $a < -b$.*

Proof.

1. For $b < 0$ and odd number p, then clearly $b^n < 0$. In the case, all roots of Eq. (6) on the complex plane are

   $$s_j = \lambda_j + a = -be^{\mathrm{i}\theta} = -b(\cos\theta_j + \mathrm{i}\sin\theta_j),$$

   where $\theta_j = (2j+1)\pi/p$, $j = 0, 1, \ldots, p-1$. The roots with largest real part are s_0 and s_{p-1}. Hence, if $a > -b\cos(\pi/p)$ is met, then $\mathrm{Re}(\lambda_j) \le \mathrm{Re}(\lambda_0) = \mathrm{Re}(s_0) - a = -b\cos(\pi/p) - a < 0$ for all $j = 0, 1, \ldots, p-1$. Further, all roots of Eq. (5) contain negative real parts when $a > -b\cos(\pi/p)$ and there are two roots s_0 and s_{p-1} having positive real parts when $a < -b\cos(\pi/p)$. Thus, the conclusion is clearly tenable.
2. Since p is an even number and $b < 0$, one has $b^n > 0$. Emphatically, the method of proof is the same as that of Lemma 3.

Case II: $\tau > 0$. Assume that there is a pair of pure virtual roots for Eq. (4) defined as $\lambda_{1,2} = \pm\mathrm{i}\omega$, we have

$$(\mathrm{i}\omega + a)^p - b^p(\cos\omega p\tau - \mathrm{i}\sin\omega p\tau) = 0.$$

Observing the above equation, we obtain

$$\begin{cases} H_1(\omega) - b^p\cos\omega p\tau = 0, \\ H_2(\omega) + b^p\sin\omega p\tau = 0, \end{cases}$$

and

$$H_1^2(\omega) + H_2^2(\omega) = b^{2p}, \tag{7}$$

where

$$H_1(\omega) = (\mathrm{i}\omega)^p + C_p^2(\mathrm{i}\omega)^{p-2}a^2 + \cdots + a^p,$$
$$\mathrm{i}H_2(\omega) = C_p^1(\mathrm{i}\omega)^{p-1}a + C_p^3(\mathrm{i}\omega)^{p-3}a^3 + \cdots + C_p^{p-1}(\mathrm{i}\omega)a^{p-1},$$

when p is an even number, and

$$H_1(\omega) = C_p^1(\mathrm{i}\omega)^{p-1}a + C_p^3(\mathrm{i}\omega)^{p-3}a^3 + \cdots + a^p,$$
$$\mathrm{i}H_2(\omega) = (\mathrm{i}\omega)^p + C_p^2(\mathrm{i}\omega)^{p-2}a^2 + \cdots + C_p^{p-1}(\mathrm{i}\omega)a^{p-1},$$

when p is an odd number.

Denoting

$$Q(\omega) \triangleq H_1^2(\omega) + H_2^2(\omega) - b^{2p} = 0,$$

then one has

$$Q(z) \triangleq z^p + \left(C_p^1 a\right)^2 z^{p-1} + \cdots + a^{2p} - b^{2p} = 0, \tag{8}$$

in which $z = \omega^2$.

Lemma 5. *Eq. (8) has at least one positive root when $a < |b|$ holds.*

Proof. If $a < |b|$ is true, then $Q(0) = a^{2p} - b^{2p} < 0$. Moreover, $Q(z)$ is a continuous function of z over $[0, \infty)$, which shows $\lim_{z\to+\infty} Q(z) = +\infty$. From the zero point theorem, there is at least one positive root for Eq. (8).

Without loss of generality, suppose that Eq. (8) has p real roots defined as z_j $(j = 1, 2, \ldots, p)$, then the corresponding frequency $\omega_j = \sqrt{z_j}$. When τ is taken as a bifurcation parameter, the key value of Hopf bifurcation point is written as

$$\tau_l^{(j)} = \frac{1}{p\omega_j}\left\{\arccos\left(\frac{H_1(\omega_j)}{b^p}\right) + 2l\pi\right\},$$

in which $j = 1, 2, \ldots, p$, $l = 0, 1, 2, \ldots$, and let

$$\tau_0 = \tau_0^{(j_0)} = \min_{j=1,2,\ldots,p}\left\{\tau_0^{(j)}\right\}, \omega_0 = \omega_{j_0}.$$

Now, we just need to check the transversality condition to ensure the generation of Hopf bifurcation. Hence, differentiating both sides of Eq. (4) with respect to τ, we have

$$p(\lambda + a)^{p-1}\frac{d\lambda}{d\tau} + b^p pe^{-\lambda p\tau}\left(\frac{d\lambda}{d\tau}\tau + \lambda\right) = 0,$$

and further

$$\left(\frac{d\lambda}{d\tau}\right)^{-1} = -\frac{1}{\lambda(\lambda + a)} - \frac{\tau}{\lambda}.$$

Substituting τ with τ_0, it follows that

$$\mathrm{Re}\left(\frac{d\lambda}{d\tau}\right)^{-1}_{\lambda=\mathrm{i}\omega_0,\tau=\tau_0} = \frac{1}{\omega_0^2 + a^2} > 0.$$

Combining with Lemma 5, the following theorem of stability and Hopf bifurcation for delayed controlled system can be derived.

Theorem 3. *For delayed controlled network (3) with one cycle, if $a < |b|$ is satisfied, then the solution of the controlled network asymptotically stabilizes to the zero equilibrium point when $\tau \in (0, \tau_0)$, and is unstable when $\tau \in (\tau_0, +\infty)$. In addition, a Hopf bifurcation occurs at the zero equilibrium point when $\tau = \tau_0$.*

3.2. Adding edges forms k non-intersected cycles

When the edge adding control forms k non-intersected cycles, and the corresponding number of nodes is defined as $q_1, q_2, \ldots, q_k$, then the subgraphs of flow graph associated with the Jacobian matrix at the zero equilibrium point has $k+1$ types, so its characteristic equation is

$$\left[(\lambda + a)e^{\lambda\tau}\right]^n - \sum_{j=1}^{k} b^{q_j}\left[(\lambda + a)e^{\lambda\tau}\right]^{n-q_j} + \sum_{j_1=1}^{k-1}\sum_{j_2=j_1+1}^{k} b^{q_{j_1}+q_{j_2}}\left[(\lambda + a)e^{\lambda\tau}\right]^{n-q_{j_1}-q_{j_2}}$$
$$+ \cdots + (-1)^k b^{\sum_{j=1}^{k} q_j}\left[(\lambda + a)e^{\lambda\tau}\right]^{n-\sum_{j=1}^{k} q_j} = 0,$$

and replacing $(\lambda + a)e^{\lambda\tau}$ by r, the equation is further rewritten as an nth polynomial equation of r

$$r^n - \sum_{j=1}^{k} b^{q_j} r^{n-q_j} + \sum_{j_1=1}^{k-1}\sum_{j_2=1}^{k} b^{q_{j_1}+q_{j_2}} r^{n-q_{j_1}-q_{j_2}} + \cdots + (-1)^k b^{\sum_{j=1}^{k} q_j} r^{n-\sum_{j=1}^{k} q_j} = 0. \tag{9}$$

Case I: $\tau = 0$. Define r_j $(j = 1, 2, \ldots, n)$ as n roots of Eq. (9) with $r = \lambda + a$, including multiple roots, then the following lemma holds.

Lemma 6. *For the controlled network (3) with k non-intersected cycles and $\tau = 0$, we have*

1. *If $a > \max_{j=1,2,\ldots,n}\{\mathrm{Re}(r_j)\}$, then network (3) is asymptotically stable at the zero equilibrium point.*
2. *If $a < \max_{j=1,2,\ldots,n}\{\mathrm{Re}(r_j)\}$, then network (3) is unstable at the zero equilibrium point.*

Proof.

1. If $a > \max\limits_{j=1,2,\dots,n}\{\mathrm{Re}(r_j)\}$ is satisfied, then we have
$$\mathrm{Re}(\lambda_j) = \mathrm{Re}(r_j) - a \le \max_{j=1,2,\dots,n}\{\mathrm{Re}(r_j)\} - a < 0,$$
which shows that all roots of the characteristic equation have negative real parts, so the zero equilibrium point of the network is asymptotically stable.
2. Define λ^* as the eigenvalue associated with $\max\limits_{j=1,2,\dots,n}\{\mathrm{Re}(r_j)\}$. If $a < \max\limits_{j=1,2,\dots,n}\{\mathrm{Re}(r_j)\}$ holds, then it is easy to verify $\mathrm{Re}(\lambda^*) = \max\limits_{j=1,2,\dots,n}\{\mathrm{Re}(r_j)\} - a > 0$. Hence, there is at least one positive root λ^*, which means that the zero equilibrium point of the network is unstable.

Case II: $\tau > 0$. Define $R_j = \alpha_j + \mathrm{i}\beta_j$ $(j = 1, 2, \dots, n)$ as n roots of Eq. (9) with $r = (\lambda + a)e^{\lambda\tau}$, including multiple roots. Hence, it holds that

$$(\lambda + a)e^{\lambda\tau} = \alpha_j + \mathrm{i}\beta_j, \tag{10}$$

for all $j = 1, 2, \dots, n$. Suppose that $\lambda_{1,2} = \pm\mathrm{i}\gamma$ $(\gamma > 0)$ is a pair of pure imaginary roots of Eq. (9), then $\lambda = \mathrm{i}\gamma$ is also the root of Eq. (10) if and only if the following equation holds

$$(\mathrm{i}\gamma + a)(\cos\gamma\tau + \mathrm{i}\sin\gamma\tau) = \alpha_j + \mathrm{i}\beta_j. \tag{11}$$

According to Eq. (11), one has

$$\begin{cases} a\cos\gamma\tau - \gamma\sin\gamma\tau = \alpha_j, \\ \gamma\cos\gamma\tau + a\sin\gamma\tau = \beta_j, \end{cases} \tag{12}$$

and

$$\varphi(\gamma) \triangleq \gamma^2 + a^2 - \alpha_j^2 - \beta_j^2 = 0, \tag{13}$$

from which we know that there exist positive real roots for Eq. (13) when $a < |R_j|$ holds. Let γ_j $(j = 1, 2, \dots, n)$ be n positive real roots of Eq. (13). By Eq. (12), the following set of critical time delay for Hopf bifurcation is obtained,

$$\tau_l^{(j)} = \frac{1}{\gamma_j}\left\{\arccos\left(\frac{a\alpha_j + \gamma_j\beta_j}{a^2 + \gamma_j^2}\right) + 2j\pi\right\},$$

with $j = 1, 2, \dots, n$, $l = 0, 1, 2, \dots$, and

$$\tau_0' = \tau_0^{(j_0)} = \min_{j=1,2,\dots,n}\left\{\tau_0^{(j)}\right\}, \gamma_0 = \gamma_{j_0}.$$

By differentiating both sides of Eq. (9) with respect to τ, the transversality condition is calculated as follows,

$$\frac{d\lambda}{d\tau}e^{\lambda\tau} + (\lambda + a)e^{\lambda\tau}\left(\frac{d\lambda}{d\tau}\tau + \lambda\right) = 0,$$

and

$$\mathrm{Re}\left(\frac{d\lambda}{d\tau}\right)^{-1}_{\lambda=\mathrm{i}\gamma_0,\tau=\tau_0'} = \frac{1}{\gamma_0^2 + a^2} > 0.$$

Therefore, we obtain the stable interval and critical delay point of the controlled network.

Theorem 4. *For delayed controlled network (3) with k non-intersected cycles, if $a < |R_j|$ $(j = 1, 2, \dots, n)$ is satisfied, then the zero equilibrium point of the network is locally asymptotically stable for $\tau \in (0, \tau_0')$, and unstable when $\tau \in (\tau_0', +\infty)$. In addition, the network undergoes a Hopf bifurcation at the zero equilibrium point when $\tau = \tau_0'$.*

Remark 3. For the intersected k cycles, the characteristic equation is more difficult to obtain, but we know that the number of terms is less than Eq. (9). In particular, if k cycles are the same size and fully intersected (see example Fig. 3), then the characteristic equation is $(\lambda + a)^{n-p}\left\{\left[(\lambda + a)e^{\lambda\tau}\right]^p - kb^p\right\} = 0$.

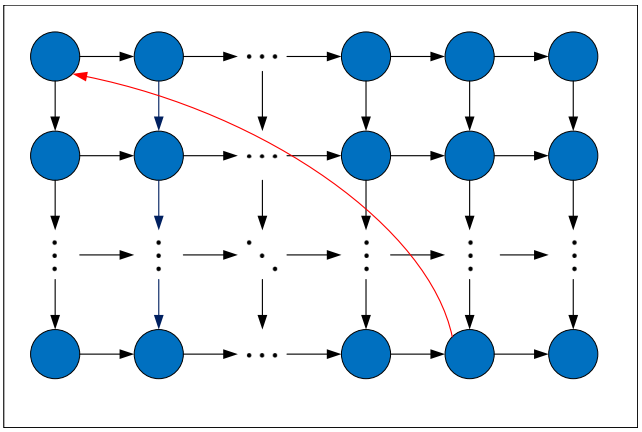

Fig. 3. Adding a reverse edge to a grid network causes the generation of multiple fully intersected cycles of the same size.

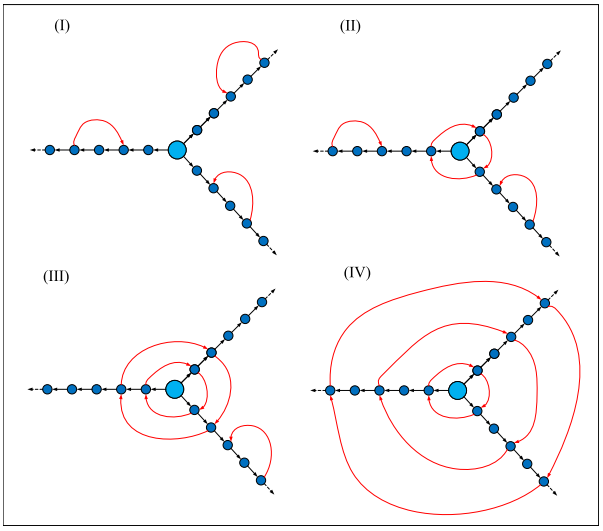

Fig. 4. Four equivalent edge adding methods have the same effect on the local dynamics of the network.

Corollary 1. *For k fully intersected cycles with the same number of nodes p, the effect of k on the first Hopf bifurcation is equivalent to revising the connection weight b in proportion.*

Proof. If adding edge control renders k fully intersected cycles with the same number of nodes p, then at zero equilibrium point, the characteristic equation of Jacobian matrix of the network is given by

$$(\lambda + a)^{n-p}\left\{\left[(\lambda + a)e^{\lambda\tau}\right]^p - kb^p\right\} = 0.$$

Hence, the critical value of time delay for the first Hopf bifurcation is

$$\tau_0^{(j_0)}(k) = \frac{\arccos\left(\frac{H_1(\omega_{j_0})}{kb^p}\right)}{p\omega_{j_0}},$$

where $\omega_{j_0}^2$ is the positive root of the following equation,

$$Q(z) \triangleq z^p + \left(C_p^1 a\right)^2 z^{p-1} + \cdots + a^{2p} - k^2b^{2p} = 0,$$

which shows that the impact of k on the first Hopf bifurcation is equivalent to increasing b by a factor of $\sqrt[p]{k}$.

Remark 4. In an undirected network, an undirected edge can be seen as a directed cycle with 2 nodes formed by two directed edges.

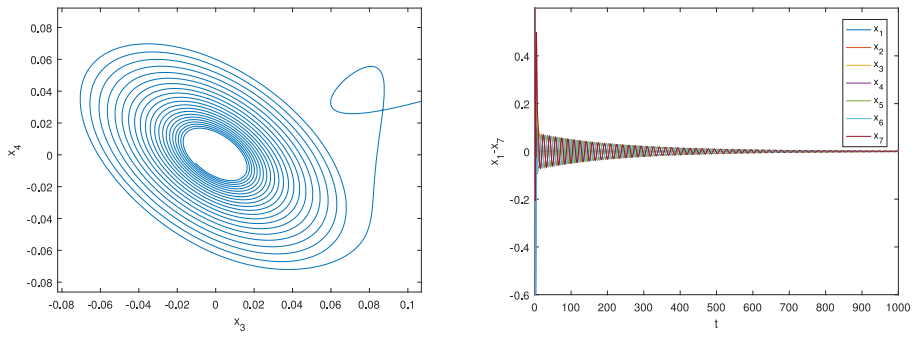

(a) $\tau = 1.3$

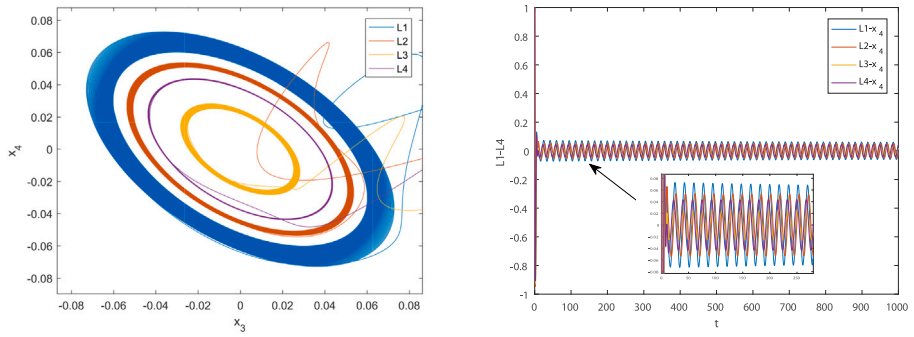

(b) $\tau = 1.41$

Fig. 5. Numerical results of network (15). (a) The zero equilibrium point of the network is locally asymptotically stable when $\tau < \tau_0$. (b) Four stable periodic solutions coexist near the zero equilibrium point when $\tau > \tau_0$, and from the inside to the outside, the initial values are (1.4,1.3,1.2,1.2,1.3,1.2,1.2), (1.5,1.3,1.1,1.2,1.3,1.1,1.2), (1.3,1.3,1.1,1,1.3,1.1,1), (1,1.3,1.1,1,1.3,1.1,1).

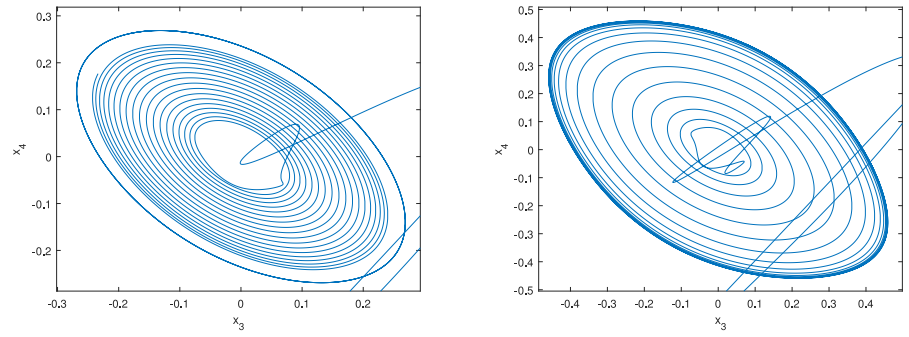

(a) $\tau = 1.6$ (b) $\tau = 2.1$

Fig. 6. Numerical results of network (15). (a)(b) With the further increase in time delay, the periodic solution near the zero equilibrium point still exists, and the periodic amplitude becomes larger and larger.

Furthermore, there are many intersected directed cycles in undirected networks. Therefore, with time delay as the bifurcation parameter, the undirected neural network would undergo Hopf bifurcation, and the bifurcation threshold is affected by the network connectivity.

4. Numerical simulation

In this section, we take the directed acyclic star-chain network as examples to display the correctness of our theoretical results. In fact, each chain of a directed acyclic star-chain network is directed, which is a more complex directed acyclic network than directed chain.

Fig. 4 shows several equivalent edge adding strategies, in which each subgraph forms three disjoint directed cycles with three nodes. According to Theorem 2, these edge adding methods have the same effect on the local dynamics of the network, that is, the Hopf bifurcation threshold of the controlled network is the same under these edge adding controls. Then, two specific examples are provided to demonstrate the impact of directed cycles on the directed neural network dynamics in the following.

Example 1 (*One Cycle*).

Consider the star-chain neural network with two nodes in each chain as

$$\begin{cases} \dot{x}_1(t) = -ax_1(t), \\ \dot{x}_2(t) = -ax_2(t) + b\tanh(x_1(t-\tau)), \\ \dot{x}_3(t) = -ax_3(t) + b\tanh(x_2(t-\tau)), \\ \dot{x}_4(t) = -ax_4(t) + b\tanh(x_1(t-\tau)), \\ \dot{x}_5(t) = -ax_5(t) + b\tanh(x_4(t-\tau)), \\ \dot{x}_6(t) = -ax_6(t) + b\tanh(x_1(t-\tau)), \\ \dot{x}_7(t) = -ax_7(t) + b\tanh(x_6(t-\tau)), \end{cases} \tag{14}$$

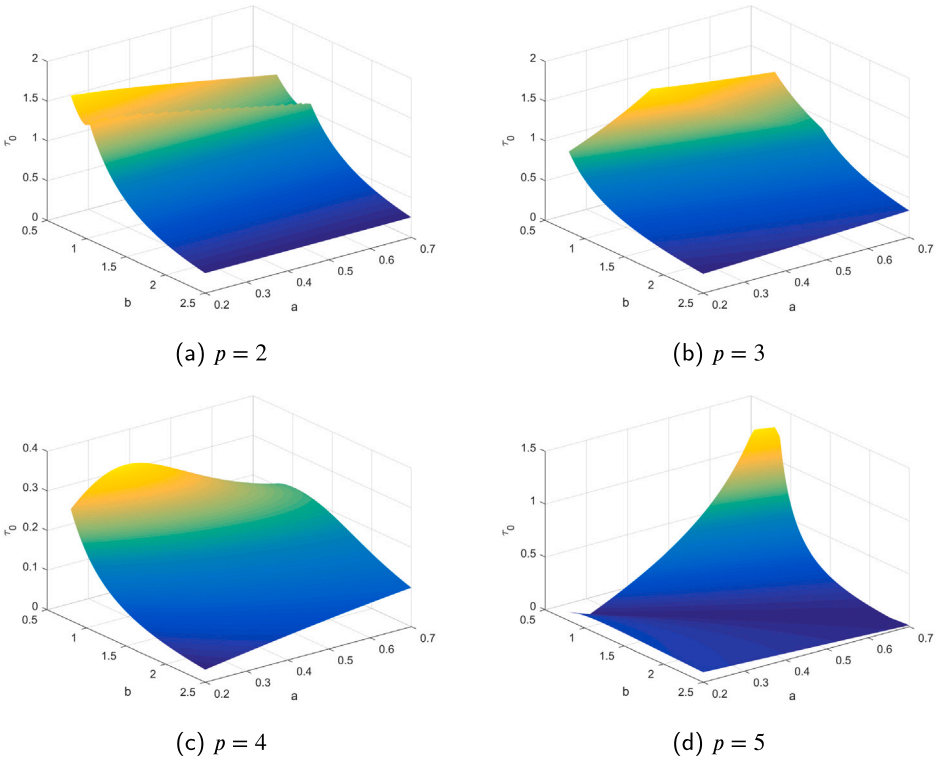

Fig. 7. Under different nodes p, bifurcation diagram of network (15) with positive connection weight b.

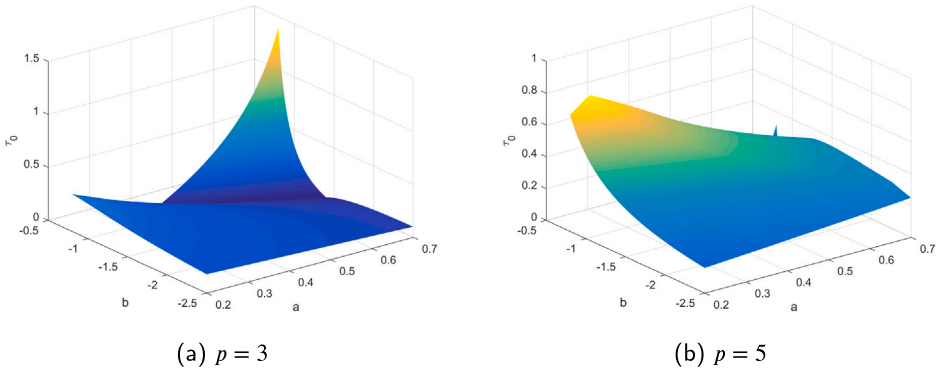

Fig. 8. Under different nodes p, bifurcation diagram of network (15) with negative connection weight b.

where the activation function is $f(x) = \tanh(x)$. It is easy to know from Lemma 1 that network (14) will not undergo Hopf bifurcation for any delay τ. Now considering the edge adding control on network (14), we get the following controlled network,

$$\begin{cases} \dot{x}_1(t) = -ax_1(t), \\ \dot{x}_2(t) = -ax_2(t) + b\tanh(x_1(t-\tau)) + b\tanh(x_4(t-\tau)), \\ \dot{x}_3(t) = -ax_3(t) + b\tanh(x_2(t-\tau)), \\ \dot{x}_4(t) = -ax_4(t) + b\tanh(x_1(t-\tau)) + b\tanh(x_6(t-\tau)), \\ \dot{x}_5(t) = -ax_5(t) + b\tanh(x_4(t-\tau)), \\ \dot{x}_6(t) = -ax_6(t) + b\tanh(x_1(t-\tau)) + b\tanh(x_2(t-\tau)), \\ \dot{x}_7(t) = -ax_7(t) + b\tanh(x_6(t-\tau)), \end{cases} \tag{15}$$

where three directed edges are added to network (14), forming a three-node directed cycle. By selecting fixed $a = 0.6$ and $b = -0.7$, the critical value $\tau_0 = 1.406$ of the first Hopf bifurcation is obtained. By Theorem 3, when $\tau < \tau_0$, the zero equilibrium point of the network is locally asymptotically stable (see Fig. 5(a)); and when $\tau > \tau_0$, periodic solutions will occur near the zero equilibrium point. It is interesting that there is a non-trivial phenomenon of four stable periodic solutions coexisting in the phase plane (see Fig. 5(b)). With the further increase in time delay, the coexistence periodic phenomenon disappears and the amplitude of the remaining single periodic solution gradually increases (see Fig. 6). It is noteworthy that the selection of initial values of phase trajectory is not mandatory and can be freely chosen within a certain range. For example, in Fig. 5(a), since the network is locally asymptotically stable with a time delay of $\tau = 1.3$, the initial values near the zero equilibrium point are feasible. However, in Fig. 5(b), there is a phenomenon of multi-period coexistence, which makes the selection range of the initial values smaller but not absolute.

Fig. 7 reflects that on the whole, the bifurcation threshold tends to decrease as the number of nodes on the cycle increases; the increase in the connection weight b can also decrease the bifurcation threshold. In addition, the self-feedback coefficient a has no significant impact on the bifurcation threshold. Therefore, under edge adding control, smaller

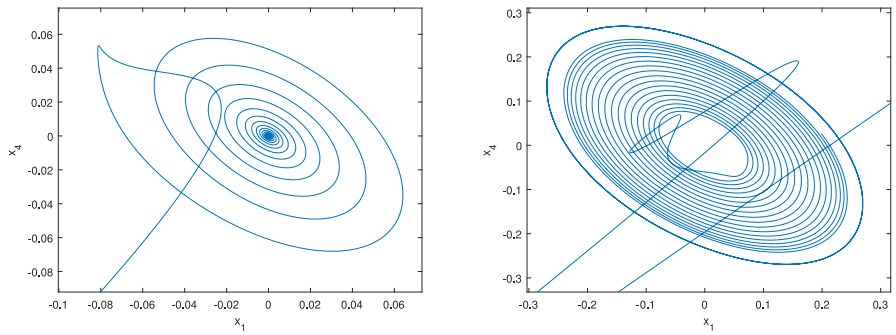

(a) $\tau = 1$ (b) $\tau = 1.6$

Fig. 9. Numerical results of network (16). (a) The zero equilibrium point of the network is locally asymptotically stable when $\tau < \tau_0'$. (b) There is a stable periodic solution near the zero equilibrium point when $\tau > \tau_0'$.

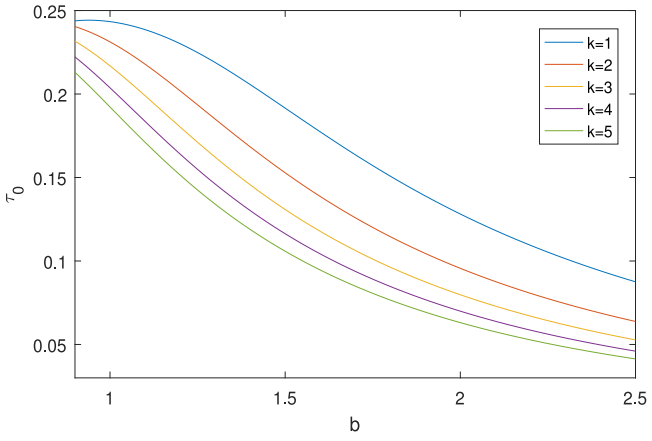

Fig. 10. Bifurcation threshold changes with the connection weight and the number of fully intersected cycles.

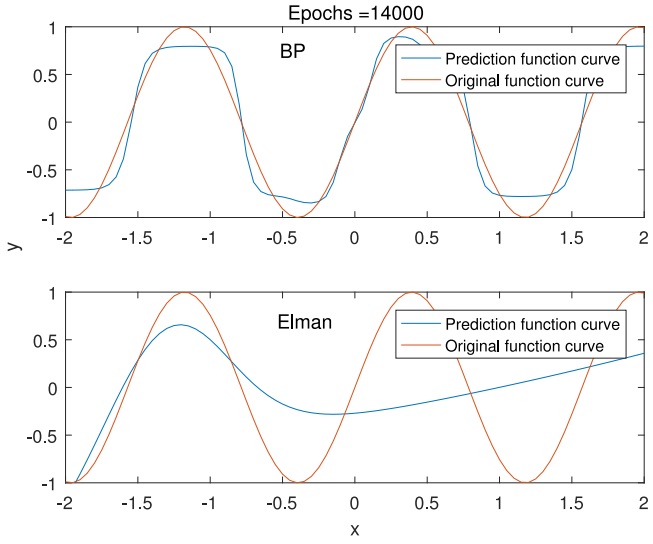

Fig. 11. Fit function $y = \sin 4x$ using BP and Elman neural networks respectively.

cycle and connection weights can effectively improve the bifurcation threshold of time delay.

Remark 5. In fact, the impact of connection weight b on the bifurcation threshold of time delay is related to the parity of the number of nodes (this is, p) on the cycle. More specifically, when p is an even number, the effects of the positive and negative b on the bifurcation threshold are consistent, but when p is an odd number, the effects are different (see Figs. 7(b)(d) and 8).

Example 2 (*Two Cycles*).

In what follows, we consider the directed cyclic neural network that forms two cycles after adding edges to network (14),

$$\begin{cases} \dot{x}_1(t) = -ax_1(t), \\ \dot{x}_2(t) = -ax_2(t) + b\tanh(x_1(t-\tau)) + b\tanh(x_4(t-\tau)), \\ \dot{x}_3(t) = -ax_3(t) + b\tanh(x_2(t-\tau)) + b\tanh(x_5(t-\tau)), \\ \dot{x}_4(t) = -ax_4(t) + b\tanh(x_1(t-\tau)) + b\tanh(x_6(t-\tau)), \\ \dot{x}_5(t) = -ax_5(t) + b\tanh(x_4(t-\tau)) + b\tanh(x_7(t-\tau)), \\ \dot{x}_6(t) = -ax_6(t) + b\tanh(x_1(t-\tau)) + b\tanh(x_2(t-\tau)), \\ \dot{x}_7(t) = -ax_7(t) + b\tanh(x_6(t-\tau)) + b\tanh(x_3(t-\tau)). \end{cases} \tag{16}$$

It is obvious that the critical value of the Hopf bifurcation is $\tau_0' = 1.295$, indicating that the zero equilibrium point of network (16) is locally asymptotically stable when $\tau = 1 < \tau_0'$ (see Fig. 9(a)), and there exists a stable periodic solution near the zero equilibrium point for $\tau = 1.6 > \tau_0'$ (see Fig. 9(b)). Moreover, Fig. 10 shows that the bifurcation threshold gradually decreases for fixed $a = 0.6$ and $p = 4$ when the connection weight and the number of fully intersected cycles increase.

A directed cyclic network can be viewed as a directed acyclic network formed cycles by adding edges. Thus, combining theoretical analysis and numerical simulations, we have the following remark.

Remark 6. In a directed neural network with time delay, cycle structure can improve the dynamic properties of the network, and the improvement in dynamics is related to the size, number, and intersection of the directed cycles.

Moreover, the results are of practical significance in some aspects. For example, we use BP (Wu, Wang, Cheng, & Li, 2011) and Elmen (with directed cycle structure) (Portegys, 2010) neural networks respectively to fit function $y = \sin 4x$. As shown in Fig. 11, it is clear that under the same epochs=14000, the fitting effect of the BP neural network is better, indicating that the cycle structure may reduce the fitting accuracy. Therefore, feedforward neural networks are commonly used to fit data. Furthermore, with the rise of graph neural network (GNN), GNN is suitable for processing large-scale graphic data. The goal of GNN is to learn useful representations from graph structured data and use these representations for various tasks. Cycle structures are widely present in real networks. As a consequence, exploring the influence of directed cycles on the stability of network model can help us further

study the recognition accuracy of GNN, which will be a potentially important research topic. We will attempt to apply the research results to practical neural network, such as GNN or GCN, in our future work.

5. Conclusion and discussion

This paper has studied the influence of adding edge on the stability of a directed acyclic neural network with time delay. It has been found that the cycle formed by edge adding operation is crucial to the dynamics of the network. Moreover, we have given the conditions for the local stability of the network and proved the existence of Hopf bifurcation with time delay as a bifurcation parameter under one cycle and multiple disjoint cycles. Numerically, a star-chain neural network model is considered, and some nontrivial phenomena are observed, such as periodic solutions and multi-periodic coexistence. Theoretical and numerical results show that edge adding control with cycle structure can effectively improve the dynamics of directed networks, and the bifurcation threshold is closely intertwined with the size of the cycle and the connection weight, and all theoretical results and numerical experiments are valid for any directed acyclic network, including directed chains, directed star-chains, and directed grids, etc.

CRediT authorship contribution statement

Qinrui Dai: Writing – original draft, Software, Methodology, Writing – review & editing. **Jin Zhou:** Methodology, Project administration, Supervision, Writing – review & editing. **Zhengmin Kong:** Project administration, Software, Visualization.

Declaration of competing interest

The authors declare that they have no known competing financial interests or personal relationships that could have appeared to influence the work reported in this paper.

Data availability

No data was used for the research described in the article.

Acknowledgments

This work was supported by the National Natural Science Foundation of China under Grant Nos. 62173254 and 62173256, by the National Key Research and Development Program of China under Grant No. 2020YFA0714200, and by the National Key R&D Program of China under Grant No. 2021ZD0112702.

References

Awodele, O., & Jegede, O. (2009). Neural networks and its application in engineering. *Informing Science and IT Education Conference(InSITE)*, 83–95.

Bang-Jensen, J., & Gutin, G. Z. (2008). *Digraphs: theory, algorithms and applications*. Springer Science & Business Media.

Chen, G., Hill, D. J., & Yu, X. (2003). *Bifurcation control: theory and applications*: *vol. 293*, Springer Science & Business Media.

Chen, J., Xiao, M., Wan, Y., Huang, C., & Xu, F. (2021). Dynamical bifurcation for a class of large-scale fractional delayed neural networks with complex ring-hub structure and hybrid coupling. *IEEE Transactions on Neural Networks and Learning Systems*.

Desoer, C. A. (1960). The optimum formula for the gain of a flow graph or a simple derivation of coates' formula. *Proceedings of the IRE*, *48*(5), 883–889.

Guan, J., Lai, R., Li, H., Yang, Y., & Gu, L. (2022). Dnrcnn: Deep recurrent convolutional neural network for hsi destriping. *IEEE Transactions on Neural Networks and Learning Systems*.

Guo, S. (2022). Theory and applications of equivariant normal forms and hopf bifurcation for semilinear FDEs in Banach spaces. *Journal of Differential Equations*, *317*, 387–421.

Hao, Y., Wang, Q., Duan, Z., & Chen, G. (2019). The role of reverse edges on consensus performance of chain networks. *IEEE Transactions on Systems, Man, and Cybernetics*, *51*(3), 1757–1765.

Jiang, X., Chen, X., Huang, T., & Yan, H. (2020). Bifurcation and control for a predator-prey system with two delays. *IEEE Transactions on Circuits and Systems II: Express Briefs*, *68*(1), 376–380.

Jiang, W., Xiong, J., & Shi, Y. (2021). A co-design framework of neural networks and quantum circuits towards quantum advantage. *Nature Communications*, *12*(1), 579.

Jiang, S., Zhou, J., Small, M., Lu, J.-a., & Zhang, Y. (2023). Searching for key cycles in a complex network. *Physical Review Letters*, *130*(18), Article 187402.

Liu, Y., Xie, D., Shi, L., & Yao, L. (2022). The effect of reverse edges on convergence rate of directed weighted chain network. *International Journal of Systems Science*, *53*(16), 3465–3480.

Mo, X., Chen, Z., & Zhang, H. (2019). Effects of adding a reverse edge across a stem in a directed acyclic graph. *Automatica*, *103*, 254–260.

Panteley, E., & Loría, A. (2017). Synchronization and dynamic consensus of heterogeneous networked systems. *IEEE Transactions on Automatic Control*, *62*(8), 3758–3773.

Papachristodoulou, A., Jadbabaie, A., & Münz, U. (2010). Effects of delay in multi-agent consensus and oscillator synchronization. *IEEE Transactions on Automatic Control*, *55*(6), 1471–1477.

Peng, Y., & Song, Y. (2009). Stability switches and hopf bifurcations in a pair of identical tri-neuron network loops. *Physics Letters A*, *373*(20), 1744–1749.

Portegys, T. E. (2010). A maze learning comparison of Elman, long short-term memory, and mona neural networks. *Neural Networks*, *23*(2), 306–313.

Premraj, D., Suresh, K., Banerjee, T., & Thamilmaran, K. (2017). Control of bifurcation-delay of slow passage effect by delayed self-feedback. *Chaos*, *27*(1), Article 013104.

Song, Y., Han, M., & Wei, J. (2005). Stability and hopf bifurcation analysis on a simplified BAM neural network with delays. *Physica D*, *200*(3–4), 185–204.

Tao, B., Xiao, M., Zheng, W. X., Cao, J., & Tang, J. (2020). Dynamics analysis and design for a bidirectional super-ring-shaped neural network with n neurons and multiple delays. *IEEE Transactions on Neural Networks and Learning Systems*, *32*(7), 2978–2992.

Wang, B., & Jian, J. (2010). Stability and hopf bifurcation analysis on a four-neuron BAM neural network with distributed delays. *Communications in Nonlinear Science and Numerical Simulation*, *15*(2), 189–204.

Wang, X., Wang, Z., & Xia, J. (2019). Stability and bifurcation control of a delayed fractional-order eco-epidemiological model with incommensurate orders. *Journal of the Franklin Institute*, *356*(15), 8278–8295.

Wang, L., Zhao, H., & Cao, J. (2016). Synchronized bifurcation and stability in a ring of diffusively coupled neurons with time delay. *Neural Networks*, *75*, 32–46.

Williams, T. C., Bach, C. C., Matthiesen, N. B., Henriksen, T. B., & Gagliardi, L. (2018). Directed acyclic graphs: A tool for causal studies in paediatrics. *Pediatric Research*, *84*(4), 487–493.

Wu, W., Wang, J., Cheng, M., & Li, Z. (2011). Convergence analysis of online gradient method for BP neural networks. *Neural Networks*, *24*(1), 91–98.

Wu, R., Zhang, C., & Feng, Z. (2021). Hopf bifurcation in a delayed single species network system. *International Journal of Bifurcation and Chaos*, *31*(03), Article 2130008.

Xu, W., Cao, J., Xiao, M., Ho, D. W., & Wen, G. (2014). A new framework for analysis on stability and bifurcation in a class of neural networks with discrete and distributed delays. *IEEE Transactions on Cybernetics*, *45*(10), 2224–2236.

Xu, Y., Ma, S., & Zhang, H. (2011). Hopf bifurcation control for stochastic dynamical system with nonlinear random feedback method. *Nonlinear Dynamics*, *65*, 77–84.

Xu, C., Tang, X., & Liao, M. (2011). Stability and bifurcation analysis of a six-neuron BAM neural network model with discrete delays. *Neurocomputing*, *74*(5), 689–707.

Yuan, L., & Yang, Q. (2015). Bifurcation, invariant curve and hybrid control in a discrete-time predator–prey system. *Applied Mathematical Modelling*, *39*(8), 2345–2362.

Zhang, H., Chen, Z., & Mo, X. (2017). Effect of adding edges to consensus networks with directed acyclic graphs. *IEEE Transactions on Automatic Control*, *62*(9), 4891–4897.

Zhou, J., Chen, J., Lu, J.-a., & Lü, J. (2016). On applicability of auxiliary system approach to detect generalized synchronization in complex network. *IEEE Transactions on Automatic Control*, *62*(7), 3468–3473.

Zhu, S., Zhou, J., Yu, X., & Lu, J.-a. (2020a). Bounded synchronization of heterogeneous complex dynamical networks: A unified approach. *IEEE Transactions on Automatic Control*, *66*(4), 1756–1762.

Zhu, S., Zhou, J., Yu, X., & Lu, J.-a. (2020b). Synchronization of complex networks with nondifferentiable time-varying delay. *IEEE Transactions on Cybernetics*, *52*(5), 3342–3348.